Jurnal Mandiri IT
Vol. 14 No. 1, July (2025), pp. 245-256

ISSN 2301-8984 (Print), 2809-1884 (Online)
Published by Institute of Computer Science

Bangka strait salinity prediction using landsat 9 oli image data

Khoirun Nisa[1], Gentio Harsono[2], Sukendra Martha[3], Dangan Waluyo[4]
[1,2,3,4] Sensing Technology Studi Program, Republic of Indonesia Defense University, Bogor, Indonesia

ARTICLE INFO

Article history:

Received Jun 30, 2025
Revised Jul 16, 2025
Accepted Jul 28, 2025

Keywords:

Bangka Strait;
Landsat 9 OLI image;
Multiple Linear Regression;
Rrs;
Salinity.

ABSTRACT

Salinity is an important parameter because it affects the environment, such as water quality, growth, and development of aquatic vegetation and various animal species. Conventional water quality monitoring is still ineffective, so it is necessary to utilize technology in monitoring water quality, including water Salinity is an important parameter because it affects the environment, such as water quality, growth, and development of aquatic vegetation and various animal species. Conventional water quality monitoring is still ineffective, so it is necessary to utilize technology in monitoring water quality, including water salinity. Utilization of remote sensing is often used to study salinity both on a small scale and a global scale. Therefore, the author conducted a study to predict salinity in the Bangka Strait using the RRS (Remote Sensing Reflectance) method. The data used are Landsat 9 OLI image data downloaded from the USGS website and in situ salinity data in the Bangka Strait sea. The Landsat 9 OLI image data used is level 2 Surface Reflectance (SR), which is ready for analysis without additional processing by the user. The data obtained were processed using multiple linear regression analysis with Rrs as the independent variable and in situ salinity as the dependent variable. Salinity prediction models are divided into three groups based on the image recording date, namely Rrs 1 for the Landsat 9 OLI image recording on May 9, 2024, Rrs 2 for July 28, 2024, and Rrs 3 for the image recording on September 28, 2023. Multiple linear regression analysis produces R^2 values for each model of 0.81662874, 0.8170285, and 0.8136894. These R^2 results indicate that the three models, Rrs 1, Rrs 2, and Rrs 3, are included in the very good criteria in predicting salinity. To choose the best of the three models, by considering the results of the validity test. The NMAE validity test for Rrs 1, Rrs 2, and Rrs 3 is 10.10152, 10.37618, and 8.88680. Meanwhile, the RMSE values are 2.41327, 2.41064, and 2.43253. Therefore, it can be determined that the Rrs 2 model is the best in predicting salinity because it has the highest R^2 value, namely 0.8170285, and the smallest RMSE, namely 2.41064.

Corresponding Author:

Khoirun Nisa,
Faculty of Engineering and Sensing Technology,
Republic of Indonesia Defense University,
IPSC Sentul Area, Sukahati, Citeureup District, Bogor Regency, West Java 16810.
Email: khoirun.samsunga11@gmail.com

1. INTRODUCTION

Salinity is an important parameter because it affects water quality, the growth and development of aquatic vegetation, and various animal species (Ansari & Akhoondzadeh, 2020). Conventional water quality monitoring involves directly observing the waters. This conventional method still fails to produce accurate results and is inefficient because visiting the waters directly requires a lot of time and effort (Wulandari et al., 2024). Therefore, alternatives are needed to monitor water quality more efficiently.

In addition to conventional methods, water quality monitoring can utilize technology. Remote sensing technology has been used to reflect the spatial distribution and dynamic changes in water quality components due to its advantages of spatial and temporal coverage (Yang et al., 2022). In terms of cost and time, remote sensing techniques are more efficient than traditional methods for assessing and measuring water quality parameters in a body of water (Abdelmalik, 2018). Water quality can be monitored routinely and effectively without spending a lot of time or money. To obtain data about the earth's surface in a constantly changing spatial and temporal scope, remote sensing solution techniques can be used. Remote sensing has been used as an alternative for monitoring water quality (Octaviana et al., 2020). One of the water quality parameters is salinity; therefore, to determine the degree of salinity of a body of water, remote sensing technology can also be used. Over the past decade, advances in L-band microwave radiometry have been made by ESA's SMOS and NASA's Aquarius and SMAP missions. These advances have demonstrated the unprecedented ability to observe global sea surface salinity (SSS) from space (Yan, 2024).

Water quality measurements are based on parameters such as pH, TDS (total dissolved solids), and salinity (Yanny, 2024). Water salinity can be analyzed using remote sensing technology (Nafizah et al., 2016). The urgent need to better monitor, understand, and constrain the ocean's role in the climate system drives SSS measurements through satellite remote sensing (Boutin et al., 2021). Remote Sensing Reflectance (Rrs) is a method that has been widely used to predict salinity. Remote Sensing Reflectance (Rrs) patterns at visible wavelengths (400–700 nm), also known as Rrs spectra, indicate the color and brightness of waters depending on the concentration of phytoplankton, CDOM, and additional particles such as mineral sediment and organic detritus (Turner et al., 2021). CDOM (Colored Dissolved Organic Matter) is a photoactive component of DOC (Dissolved Organic Carbon), which is the most dominant source of organic carbon in aquatic ecosystems (Ciancia et al., 2023). To what extent and how well does this method, along with sensing technology data such as Landsat imagery, provide information about the salinity of waters? Therefore, a study is needed to discuss this and how the salinity prediction model performs in predicting salinity.

Research (Ansari & Akhoondzadeh, 2020) conducted radiometric and atmospheric corrections to obtain surface reflectance (SR) images. This study used Landsat 9 OLI level 2 Surface Reflectance (SR) image data. The Committee on Earth Observation Satellites (CEOS) recognizes Landsat Collection 2 science products as Analysis Ready Data (ARD). Satellite data that has been processed with minimal requirements and organized in a way that allows direct analysis with minimal user effort receives this certification. It also allows interoperability with other datasets over time (U.S. Geological Survey, n.d.). Departing from several problems that occur, especially the difficulty and inefficiency of conventional water quality monitoring, this study was conducted with the aim of predicting sea surface salinity from remote sensing reflectance (Rrs) and Landsat 9 OLI level 2 Surface Reflectance (SR) imagery and how the resulting prediction model performs. The Geological Glossary (Neuendorf et al., 2005) defines a strait as a relatively narrow waterway connecting two larger bodies of water (Rossi et al., 2023). The Bangka Strait lies between the east coast of South Sumatra Island and Bangka Island. A significant amount of freshwater enters the Bangka Strait through large rivers along the east coast of South Sumatra, particularly in Banyuasin Regency and Ogan Komering Ilir Regency, which flow into the Bangka Strait. Freshwater from these upstream rivers mixes with seawater, impacting water dynamics and quality (Surbakti et al., 2022). In this study, a multiple linear regression algorithm was used to predict sea surface salinity from Rrs using in-situ measurements collected in the Bangka region. Combined with Landsat 9 OLI imagery data downloaded from earthexplorer.usgs.gov, field salinity data, or in-situ salinity, were analyzed to develop a salinity prediction model.

2. RESEARCH METHOD

The research area is centered in the Bangka Strait. According to (Rahma et al., 2024), the Bangka Strait is a body of water located between the islands of Sumatra and Bangka. Field or in situ salinity sampling was conducted at 11 points, then selected and aligned with the position of the Landsat 9 OLI imagery obtained. The downloaded Bangka Strait imagery data was Landsat 9 OLI Surface Reflectance (SR) imagery. Sharaf El Din et al. created an algorithm to calculate turbidity and total suspended solids using Landsat 8 surface reflectance data (Jin et al., 2023). Quantitative method s were used in this study with the following design :

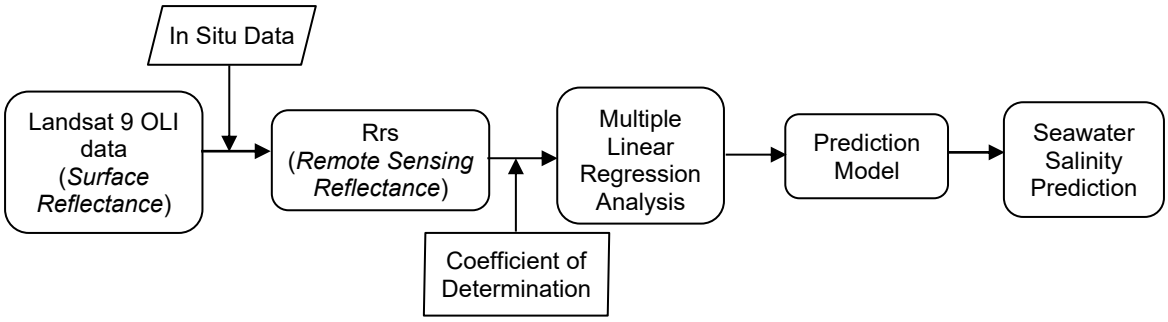

Figure 1. Research Design

Based on the introduction and research design, it can be seen that the population of the study is the seawater of the Bangka Strait, and the salinity of the seawater is the target of the study (sample). Landsat 9 OLI image data was downloaded from the USGS website in three groups of image data based on the time of image recording and processing, as shown in Table 1 below :

Table 1. Landsat 9 OLI Image Data

Name	Recording Date	Processing Date
LC09_L2SP_124061_20240509_20240511_02_T1	2024-05-09	2024-05-11
LC09_L2SP_124061_20240728_20240729_02_T1	2024-07-28	2024-07-29
LC09_L2SP_124061_20230928_20230930_02_T1	2023-09-28	2023-09-30

The bands used in Landsat 9 OLI imagery are Band 2 (450 nm-515 nm), Band 3 (525 nm-600 nm), and Band 4 (630 nm-680 nm), in accordance with research conducted by (Meng et al., 2022). Field data consists of seawater salinity values taken directly from 11 water samples from the Bangka Strait. However, due to signal interference, 10 seawater sample points were used. Field salinity values were measured using a salinity refractometer, as in research conducted by (Yoshii et al., 2025). The unit of salinity measurement is ppt (parts per thousand). PPT (parts per thousand) is the number of parts or grams of salt in one kilogram (1000 grams) of seawater (Alatawi, 2022). The results of in situ salinity measurements are shown in Table 2 below :

Table 2. Salinity of Seawater in the Bangka Strait (Coordinate Selection)

STA	Latitude	Longitude	Time Capture	Salinity (ppt)
1	2°20’58”S	104°54’25”E	11:32:56	5
2	2°22’9”S	104°48’13”E	13:01:54	14
3	2°19’51”S	104°49’24”E	14:17:16	15
4	2°21’56”S	104°50’39”E	15:24:11	7
5	2°11’56”S	104°55’40”E	16:07:41	15
6	2°9’34”S	105°0’34”E	16:32:52	20
7	2°5’1”S	105°7’56”E	18:29:21	30
8	2°6’14”S	105°7’20”E	19:32:31	25
9	2°8’9”S	105°2’55”E	20:15:21	16
10	2°10’37”S	104°57’47”E	21:08:09	0

After 10 samples were measured for salinity, there was 1 point that did not match, namely at STA 10 with coordinates 2°10'37"S and 104°57'47"E (located in the ocean), the salinity measurement results were 0. This was likely due to an error in taking seawater samples at that point, so the water sample at STA 10 was not used. So for the Rrs calculation, 9 salinity sample points were used.

Table 3. Salinity of Bangka Strait Seawater Salinity (Salinity Selection)

STA	Latitude	Longitude	Latitude	Longitude	Salinity (ppt)
1	2°20'58"S	104°54'25"E	-2.34944	104.90694	5
2	2°22'9"S	104°48'13"E	-2.36917	104.80361	14
3	2°19'51"S	104°49'24"E	-2.33083	104.82333	15
4	2°21'56"S	104°50'39"E	-2.36556	104.84417	7
5	2°11'56"S	104°55'40"E	-2.19889	104.92778	15
6	2°9'34"S	105°0'34"E	-2.15944	105.00944	20
7	2°5'1"S	105°7'56"E	-2.08361	105.13222	30
8	2°6'14"S	105°7'20"E	-2.10389	105.12222	25
9	2°8'9"S	105°2'55"E	-2.13583	105.04861	16

Multiple linear regression analysis using nine field salinity samples according to Table 3. Where the field salinity value is the dependent variable and Rrs (Remote Sensing Reflectance) is the independent variable. The Rrs formula (Novoa et al., 2017) can be expressed as follows :

$$Rrs = \frac{\rho}{\pi} \quad (1)$$

ρ is the reflectance value of water leaving a dimensionless space. Archimedes (287–212 BC) calculated PI (π) and gave an estimated value of 3.14159 (Dewangan, 2023). The multiple linear regression prediction equation (Sahbeni, 2021) is stated as :

$$Y = A_0 + A_1 . x_1 + A_2 . x_2 + A_3 . x_3 + \ldots A_n . x_n \quad (2)$$

where Y is the dependent variable, xi is the explanatory variable, Ai is the coefficient of variable i, and A0 is the intercept.

3. RESULTS AND DISCUSSIONS

Calculation of Remote Sensing Reflectance (Rrs) for each Landsat 9 OLI image recording date using the QGIS Raster Calculator tool. Since the scale factor for Landsat imagery is 0.00001 (U.S. Geological Survey, 2025), in the Rrs calculation using the raster calculator, the image band is divided by 10000 and then divided by the value of π. The calculated Rrs display in GeoTIFF (raster) format is as follows :

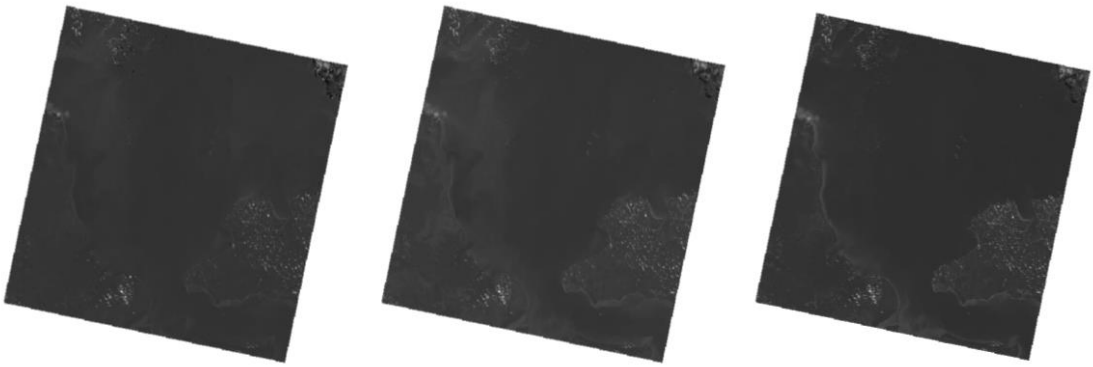

Figure 2. Rrs 1 (2024-05-09) : (a) Rrs band 2; (b) Rrs band; Rrs band 4

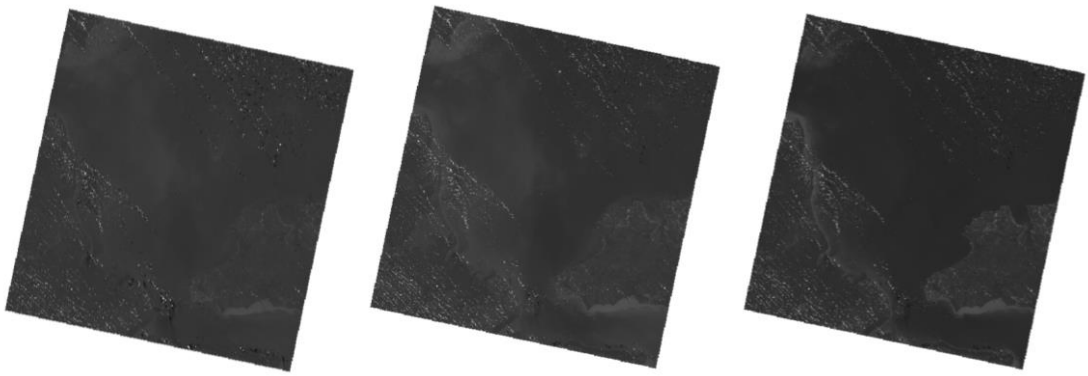

Figure 3. Rrs 2 (2024-07-28) : (a) Rrs band 2; (b) Rrs band; Rrs band 4

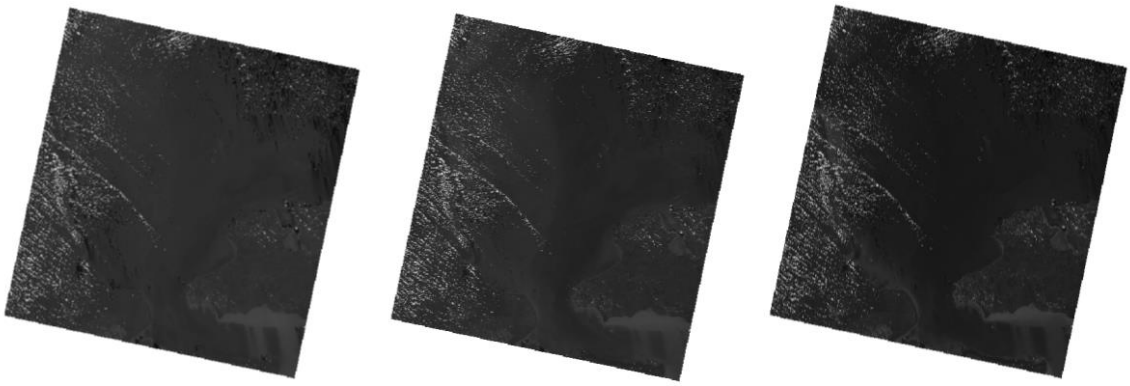

Figure 4. Rrs 3 (2023-09-28) : (a) Rrs band 2; (b) Rrs band; Rrs band 4

The Rrs raster was extracted to obtain the Rrs values at the sampling coordinate points. The results showed that only five sampling points could be extracted, with the remaining four points being labeled NULL, meaning empty. After obtaining the Rrs values for each band and at each sampling point, multiple linear regression analysis was performed to obtain several parameters that would then become components of the equation for predicting seawater salinity. The analysis was performed using Microsoft Excel.

Table 4. Results of Rrs extraction for each image band at sampling point Rrs 1

STA	Latitude	Longitude	Salinity	Rrs b2	Rrs b3	Rrs b4
5	-2.19900	104.92800	15	0.262765	0.308984	0.323212
6	-2.15900	105.00900	20	0.242393	0.256558	0.244653
7	-2.08400	105.13200	30	0.341547	0.378503	0.385856
8	-2.10400	105.12200	25	0.240388	0.245958	0.234626
9	-2.13600	105.04900	16	0.249078	0.258500	0.244749

Table 5. Results of Rrs extraction for each image band at Rrs sampling point 2

STA	Latitude	Longitude	Salinity	Rrs b2	Rrs b3	Rrs b4
5	-2.19900	104.92800	15	0.239560	0.290649	0.269068
6	-2.15900	105.00900	20	0.213140	0.262288	0.226000
7	-2.08400	105.13200	30	0.352592	0.378375	0.389452
8	-2.10400	105.12200	25	0.260887	0.290426	0.241470
9	-2.13600	105.04900	16	0.252897	0.267667	0.232462

Table 6. Results of Rrs extraction for each image band at Rrs sampling point 3

STA	Latitude	Longitude	Salinity	Rrs b2	Rrs b3	Rrs b4
5	-2.19900	104.92800	15	0.235900	0.316825	0.277344
6	-2.15900	105.00900	20	0.267253	0.302934	0.241661
7	-2.08400	105.13200	30	0.366884	0.395372	0.407119
8	-2.10400	105.12200	25	0.269163	0.301949	0.254234
9	-2.13600	105.04900	16	0.266903	0.287358	0.249364

Table 7. Summary of Data Analysis Results

Parameter	Rrs 1	Rrs 2	Rrs 3
Constant (α)	0.94438083	-51.34283	-42.014059
β band 2	971.26747	-14.75954	140.05767
β band 3	-1656.2311	494.74135	212.98719
β band 4	839.129751	-261.0965	-155.68756
R^2	0.81662874	0.8170285	0.8136894

Several parameters obtained from the analysis results are then entered into equation (3), namely the multiple linear regression equation or salinity prediction equation. Calculation of seawater salinity prediction is grouped based on the satellite image recording date, namely Rrs 1 for image recording on May 9, 2024, Rrs 2 for image recording on July 28, 2024, and Rrs 3, whose image was recorded on September 28, 2023. In the study of oil palm yield prediction using Landsat-7 satellite data, for deeper condition networks, the highest overall prediction accuracy was obtained, namely 0.79, 0.77, and 0.85 (Ang et al., 2025).

.

Table 8. Classification of Statistical Index (R^2)

R^2 Value Range	Criteria
$R^2 \leq 0.25$	It is not in accordance with
$0.25 < R^2 \leq 0.50$	Bad
$0.50 < R^2 \leq 0.60$	Average
$0.60 < R^2 \leq 0.75$	Good
$0.75 < R^2 \leq 1.00$	Sangat Baik

Because the salinity prediction calculations are grouped into three based on image recording, the prediction models are also grouped into three. The salinity prediction results are based on calculations using multiple linear regression equations, using the numbers from the parameters obtained from the analysis and combined with the Remote Sensing Reflectance (Rrs) values for the bands in the Landsat 9 OLI image that have been previously determined. These bands are band 2 (blue band), band 3 (green band), and the red band (band 4).

In the tabulation of salinity prediction calculations, the descriptions for the Remote Sensing Reflectance (Rrs) values for each band are Rrs Band 2, which explains the Rrs value for the blue band (band 2); Rrs Band 3 for the Rrs value for the green band (band 3); and Rrs Band 5, which refers to the value of the Rrs for the red band (band 5).

Table 9. Predicted Seawater Salinity Rrs 1

STA	In situ Salinity	Rrs Band 2	Rrs Band 3	Rrs Band 4	Salinity Prediction (ppt)
5	15	0.262765	0.308984	0.323212	15.6281
6	20	0.242393	0.256558	0.244653	16.7495
7	30	0.341547	0.378503	0.385856	29.5728
8	25	0.240388	0.245958	0.234626	23.9436
9	16	0.249078	0.258500	0.244749	20.1061

Table 10. Predicted Seawater Salinity Rrs 2

STA	In situ Salinity	Rrs Band 2	Rrs Band 3	Rrs Band 4	Salinity Prediction (ppt)
5	15	0.239560	0.290649	0.269068	18.66484
6	20	0.213140	0.262288	0.226000	16.26795
7	30	0.352592	0.378375	0.389452	28.96629
8	25	0.260887	0.290426	0.241470	25.44545
9	16	0.252897	0.267667	0.232462	16.65546

Table 11. Predicted Seawater Salinity Rrs 3

STA	In situ Salinity	Rrs Band 2	Rrs Band 3	Rrs Band 4	Salinity Prediction (ppt)
5	15	0.235900	0.316825	0.277344	15.32623
6	20	0.267253	0.302934	0.241661	22.31424
7	30	0.366884	0.395372	0.407119	30.19671
8	25	0.269163	0.301949	0.254234	20.41435
9	16	0.266903	0.287358	0.249364	17.74847

Table 12. Summary of Predicted Seawater Salinity in the Bangka Strait

STA	In situ Salinity	Salinity Prediction (ppt)		
		Rrs 1	Rrs 2	Rrs 3
5	15	15.6281	18.66484	15.32623
6	20	16.7495	16.26795	22.31424
7	30	29.5728	28.96629	30.19671
8	25	23.9436	25.44545	20.41435
9	16	20.1061	16.65546	17.74847

From the three seawater salinity prediction tables above, it can be seen that each shows figures that are not significantly different from the field (in situ) salinity figures. Hypothesis testing in multiple linear analysis can be performed using three methods: individual parameter significance testing (t-test), simultaneous significance testing (F-test), and coefficient of determination (R2) testing (Fitri et al., 2024). A summary of the hypothesis testing results is shown in Table 13 below :

Table 13. Hypothesis Test Results

Hypothesis Test Parameters	Rrs 1	Rrs 2	Rrs 3
R^2	0.81662874	0.8170285	0.8136894
Sig. F	0.52807055	0.52753309	0.5320001
P-value (α)	0.97921554	0.47182896	0.5974522
P-value (Rrs band 2)	0.43592000	0.94957697	0.4546666
P-value (Rrs band 3)	0.53578855	0.48258268	0.6717292
P-value (Rrs band 4)	0.58116999	0.49174011	0.6427575

Simultaneous significance test (F test): namely, the significant F value on Rrs 1, Rrs 2, and Rrs 3 is 0.52807055017078, 0.5275330940124890, and 0.5320001639797650, which means the model is not feasible (Sig > α (5%)). Likewise, the value produced in the individual parameter significance test (t-test), each variable Rrs band 2, Rrs band 3, and Rrs band 4, produces a P-value > 0.05; this indicates that there is no partial influence between the independent variable and the dependent variable. While the coefficient of determination (R^2) test on each prediction model, Rrs 1, Rrs 2, and Rrs 3, produces a number close to one, in other words, almost all the data needed to predict the variation of the dependent variable is provided by the independent variables.

Validity testing uses the NMAE (normalized mean absolute error) method. To obtain the NMAE value, you can use the following formula :

$$NMAE = \frac{1}{n}\sum_{i=1}^{n}\frac{|Yi-Y'i|}{\sqrt{Yi\,.Y'i}} \quad (3)$$

According to (Zhao et al., 2022), Yi and Y'i are the actual and predicted values in time period i, and n is the test data set.

Table 14. Results of NMAE Rrs 1 Calculation

STA	Salinitas		|Yi - Y'i|	$\sqrt{\text{Yi.Y'i}}$	$\frac{\lvert Yi - Y'i\rvert}{\sqrt{(\text{Yi.Y'i})}}$
	In situ (Yi)	Prediction (Y'i)			
5	15	15.628	0.628068	15.31081	0.04102122
6	20	16.749	3.250531	18.30271	0.17759832
7	30	29.573	0.427225	29.78562	0.01434335
8	25	23.944	1.056445	24.46608	0.04317999
9	16	20.106	4.106134	17.93595	0.22893322
NMAE					0.10101522
NMAE (%)					10.10152205

Table 15. Results of NMAE Rrs 2 Calculations

STA	Salinitas		|Yi - Y'i|	$\sqrt{\text{Yi.Y'i}}$	$\frac{\lvert Yi - Y'i\rvert}{\sqrt{(\text{Yi.Y'i})}}$
	In situ (Yi)	Prediction (Y'i)			
5	15	15.628	3.664843	16.73238	0.21902695
6	20	16.749	3.732049	18.03771	0.2069026
7	30	29.573	1.033706	29.47862	0.03506631
8	25	23.944	0.445451	25.22174	0.01766138
9	16	20.106	0.655462	16.32444	0.04015217
NMAE					0.103761882
NMAE (%)					10.37618825

Table 16. Results of NMAE Rrs 3 Calculation

STA	Salinitas		|Yi - Y'i|	$\sqrt{\text{Yi.Y'i}}$	$\frac{\lvert Yi - Y'i\rvert}{\sqrt{(\text{Yi.Y'i})}}$
	In situ (Yi)	Prediction (Y'i)			
5	15	15.326	3.664843	16.73238	0.021516
6	20	22.314	3.732049	18.03771	0.109548
7	30	30.197	1.033706	29.47862	0.006536
8	25	20.414	0.445451	25.22174	0.202984
9	16	17.748	0.655462	16.32444	0.103757
NMAE					0.088868
NMAE (%)					8.886803

In addition to using NMAE, the validity test also uses RMSE (Root Mean Square Error). The RMSE equation can be expressed by Equation (4) (Hodson, 2022).

$$\text{RMSE} = \sqrt{\frac{1}{n}\sum_{1}^{n}(yi - \hat{y}i)^2} \quad (4)$$

Where n is the number of observations in the validation data set (number of data), yi is the observed value in the validation data (actual value), and ŷi is the predicted value.

Table 17. Results of RMSE Calculation Rrs 1

STA	Salinitas		(Yi - Y'i)	(Yi - Y'i)²
	In situ	Prediction		

5	15	15.628	-0.62807	0.39447
6	20	16.749	3.250531	10.56595
7	30	29.573	0.427225	0.182522
8	25	23.944	1.056445	1.116076
9	16	20.106	-4.10613	16.86033
Rata - rata (Yi - Y'i)²				5.823871
RMSE				2.41327

Table 18. Results of RMSE Calculation Rrs 2

STA	Salinitas		(Yi - Y'i)	(Yi - Y'i)²
	In situ	Prediction		
5	15	18.665	-3.66484	13.43107
6	20	16.268	3.732049	13.92819
7	30	28.966	1.033706	1.068549
8	25	25.445	-0.44545	0.198426
9	16	16.655	-0.65546	0.42963
Rata - rata (Yi - Y'i)²				5.811174
RMSE				2.410638

Table 19. Results of RMSE Calculation Rrs 3

STA	Salinitas		(Yi - Y'i)	(Yi - Y'i)²
	In situ	Prediction		
5	15	15.326	-0.32623	0.106423
6	20	22.314	-2.31424	5.355721
7	30	30.197	-0.19671	0.038695
8	25	20.414	4.585645	21.02814
9	16	17.748	-1.74847	3.057134
Rata - rata (Yi - Y'i)²				5.917223
RMSE				2.432534

The NMAE validity test for Rrs 1, Rrs 2, and Rrs 3 is 10.10152, 10.37618 and 8.88680. Meanwhile, the RMSE value is 2.41327, 2.41064 and 2.43253. To see the comparison between these two validity test values, the relationship between the two can be illustrated through the following diagram :

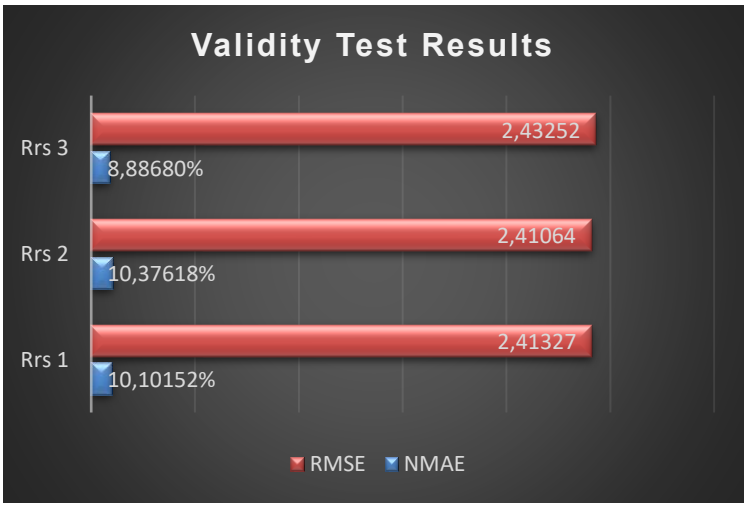

Figure 5. Validity Test Results Chart

The closer the RMSE is to zero, the better the correlation in estimating the desired parameters (Tuc et al., 2025). In their study, (Fkih, 2022) stated that the closer the MAE, NMAE, and

RMSE are to 0, the better the performance of the recommendation system. Therefore, it can be stated that the smaller the RMSE and NAME values (closer to zero), the better the model is in predicting. Research (Muhsi et al., 2022) produced a NMAE value of 0.47% and RMSE = 0.17, indicating that the developed algorithm model is adequate for estimating sea surface salinity values. Meanwhile, in this study, the average NMAE and RMSE values have a significant difference from the previously mentioned study. This is because the number of in situ data that can be used in this study is only 5 data, while previous research has around 10 data. This is supported by research (Hoffman, 2021), where of the 6 tables that list RMSE, there are 4 tables that show the largest RMSE values obtained from the fewest number of observation data. However, this study has an average R^2 value of 0.8, this is within the range of R^2 results produced from research on oil palm yield prediction using Landsat-7 satellite data, for deeper condition networks resulting in the highest overall prediction accuracy of 0.79, 0.77 and 0.85 (Ang et al., 2025).

4. CONCLUSION

The results of the study indicate that the salinity prediction model performs well in predicting seawater salinity, as indicated by the resulting R^2 value. The average R^2 generated from the three models is 0.8. A salinity prediction model utilizing sensing technology will facilitate water salinity monitoring. This will support seawater management, for example, in the planning of desalination installations to utilize seawater as a raw water source. Future research can use other imagery in predicting salinity, for example, using MODIS (Moderate Resolution Imaging Spectroradiometer) imagery.

REFERENCES

Abdelmalik, K. W. (2018). Role of statistical remote sensing for Inland water quality parameters prediction. Egyptian Journal of Remote Sensing and Space Science, 21(2), 193–200. https://doi.org/10.1016/j.ejrs.2016.12.002

Alatawi, A. S. (2022). A Testbed for Investigating the Effect of Salinity and Turbidity in the Red Sea on White-LED-Based Underwater Wireless Communication. Applied Sciences (Switzerland), 12(18). https://doi.org/10.3390/app12189266

Ang, Y., Shafri, H. Z. M., Lee, Y. P., Bakar, S. A., Abidin, H., Hashim, S. J., Samad, M. N., Che'ya, N. N., Hassan, M. R., Lim, H. S., Abdullah, R., Yusup, Y., Muhammad, S. A., Yin, T. S., & Gibril, M. B. A. (2025). Block-scale Oil Palm Yield Prediction Using Machine Learning Approaches Based on Landsat and MODIS Satellite Data. Journal of Advanced Research in Applied Sciences and Engineering Technology, 45(1), 90–107. https://doi.org/10.37934/araset.45.1.90107

Ansari, M., & Akhoondzadeh, M. (2020). Mapping water salinity using Landsat-8 OLI satellite images (Case study: Karun basin located in Iran). Advances in Space Research, 65(5), 1490–1502. https://doi.org/10.1016/j.asr.2019.12.007

Boutin, J., Reul, N., Koehler, J., Martin, A., Catany, R., Guimbard, S., Rouffi, F., Vergely, J. L., Arias, M., Chakroun, M., Corato, G., Estella-Perez, V., Hasson, A., Josey, S., Khvorostyanov, D., Kolodziejczyk, N., Mignot, J., Olivier, L., Reverdin, G., … Mecklenburg, S. (2021). Satellite-Based Sea Surface Salinity Designed for Ocean and Climate Studies. Journal of Geophysical Research: Oceans, 126(11), 1–28. https://doi.org/10.1029/2021JC017676

Ciancia, E., Campanelli, A., Colonna, R., Palombo, A., Pascucci, S., Pignatti, S., & Pergola, N. (2023). Improving Colored Dissolved Organic Matter (CDOM) Retrievals by Sentinel2-MSI Data through a Total Suspended Matter (TSM)-Driven Classification: The Case of Pertusillo Lake (Southern Italy). Remote Sensing, 15(24). https://doi.org/10.3390/rs15245718

Dewangan, L. (2023). The Exact Measurement of Pi. International Journal for Research in Applied Science and Engineering Technology, 11(8), 2217–2233. https://doi.org/10.22214/ijraset.2023.55555

Fitri, N. L., Pangaribuan, D., & Yuniati, T. (2024). Pengaruh Free Cash Flow, Investment Opportunity Set, Dan Struktur Modal Terhadap Kebijakan Dividen Pada Perusahaan Food and Beverage. *SENTRI: Jurnal Riset Ilmiah*, *3*(2), 740–760. https://doi.org/10.55681/sentri.v3i2.2324

Fkih, F. (2022). Similarity measures for Collaborative Filtering-based Recommender Systems: Review and experimental comparison. Journal of King Saud University - Computer and Information Sciences, 34(9), 7645–7669. https://doi.org/10.1016/j.jksuci.2021.09.014

Hodson, T. O. (2022). Root-mean-square error (RMSE) or mean absolute error (MAE): when to use them or not. Geoscientific Model Development, 15(14), 5481–5487. https://doi.org/10.5194/gmd-15-5481-2022

Hoffman, S. (2021). Estimation of prediction error in regression air quality models. *Energies*, *14*(21). https://doi.org/10.3390/en14217387

Jin, H., Fang, S., & Chen, C. (2023). Mapping of the Spatial Scope and Water Quality of Surface Water Based on the Google Earth Engine Cloud Platform and Landsat Time Series. Remote Sensing, 15(20), 1–21. https://doi.org/10.3390/rs15204986

Keer, M., Lohiya, H., & Chouhan, S. (2023). Goodness of Fit for Linear Regression using R squared and Adjusted R-Squared. International Journal of Research Publication and Reviews Journal Homepage: Www.Ijrpr.Com, 4(3), 2431–2439. www.ijrpr.com

Kim, H.-Y. (2019). Statistical notes for clinical researchers: simple linear regression 3 – residual analysis. Restorative Dentistry & Endodontics, 44(1), 1–8. https://doi.org/10.5395/rde.2019.44.e11

Li, J. (2017). Assessing the accuracy of predictive models for numerical data: Not r nor r2, why not? Then what? PLoS ONE, 12(8), 1–16. https://doi.org/10.1371/journal.pone.0183250

Meng, H., Zhang, J., & Zheng, Z. (2022). Retrieving Inland Reservoir Water Quality Parameters Using Landsat 8-9 OLI and Sentinel-2 MSI Sensors with Empirical Multivariate Regression. International Journal of Environmental Research and Public Health, 19(13). https://doi.org/10.3390/ijerph19137725

Nafizah, Jaelani, L. M., & Winarso, G. (2016). Garam 3. Jurnal Tehnik Its, 5(September).

Novoa, S., Doxaran, D., Ody, A., Vanhellemont, Q., Lafon, V., Lubac, B., & Gernez, P. (2017). Atmospheric corrections and multi-conditional algorithm for multi-sensor remote sensing of suspended particulate matter in low-to-high turbidity levels coastal waters. Remote Sensing, 9(1). https://doi.org/10.3390/rs9010061

Octaviana, A., Prasetyo, Y., & Amarrohman, F. J. (2020). Analisis perubahan nilai total suspended solid tahun 2016 Dan 2019 menggunakan citra sentinel 2a (Studi Kasus : Banjir Kanal Timur, Semarang). Jurnal Geodesi Undip, 9(2), 167–176.

Rahma, A. A., Adrianto, D., & Malik, K. (2024). Pemodelan Numerik Arus Pasang Surut 2D Menggunakan Software Mike 21 (Studi Kasus Selat Bangka). Jurnal Hidrografi Indonesia, 4(2), 87–94. https://doi.org/10.62703/jhi.v4i2.36

Rossi, V. M., Longhitano, S. G., Olariu, C., & Chiocci, F. L. (2023). Straits and seaways: controls, processes and implications in modern and ancient systems. Geological Society Special Publication, 523(1), 1–15. https://doi.org/10.1144/SP523-2022-271

Sahbeni, G. (2021). Soil salinity mapping using Landsat 8 OLI data and regression modeling in the Great Hungarian Plain. SN Applied Sciences, 3(5), 1–13. https://doi.org/10.1007/s42452-021-04587-4

Surbakti, H., Nurjaya, I. W., Bengen, D. G., & Prartono, T. (2022). Kontribusi Massa Air Tawar dari Estuari Banyuasin ke Perairan Selat Bangka pada Musim Peralihan II. Positron, 12(1), 29. https://doi.org/10.26418/positron.v12i1.53035

Tuc, E., Akbas, S. O., & Babagiray, G. (2025). Reliability and Validity Analysis of Correlations on Strength and Consolidation Parameters for Ankara Clay and Proposal for a New Correlation. Arabian Journal for Science and Engineering, 50(11), 8107–8126. https://doi.org/10.1007/s13369-024-09181-5

Turner, J. S., Friedrichs, C. T., & Friedrichs, M. A. M. (2021). Long-Term Trends in Chesapeake Bay Remote Sensing Reflectance: Implications for Water Clarity. Journal of Geophysical Research: Oceans, 126(12). https://doi.org/10.1029/2021JC017959

Wulandari, S. A., Sucipto, A., Rosyady, A. F., Ardana, M. D. R., Cahyono, O. D. P., & Khomarudin, A. N. (2024). Rancang Bangun Sistem Monitoring Kualitas Air Untuk Mendeteksi Keadaan Tidak Normal atau Penyakit Pada Tambak Ikan Mujaer Menggunakan Fuzzy Logic Mamdani Berbasis Mobile. Technologica, 3(1), 42–54. https://doi.org/10.55043/technologica.v3i1.153

Yan, L. (2024). Ocean salinity. Nature Climate Change, 14(4), 309. https://doi.org/10.1038/s41558-024-01987-3

Yang, H., Kong, J., Hu, H., Du, Y., Gao, M., & Chen, F. (2022). A Review of Remote Sensing for Water Quality Retrieval: Progress and Challenges. Remote Sensing, 14(8). https://doi.org/10.3390/rs14081770

Yanny. (2024). Pengukuran Kualitas Air Sumur (pH, TDS, Salinitas) di Desa Matsa Halmahera Utara. Jurnal Pengabdian Kepada Masyarakat, 1, 20–26.

Yoshii, K., Takayanagi, H., Miyajima, T., Reuning, L., Yamamoto, K., & Iryu, Y. (2025). Origin of interstitial water beneath the continental shelf offshore northwestern Australia: insights from hydrogen and oxygen isotope compositions. Progress in Earth and Planetary Science, 12(1). https://doi.org/10.1186/s40645-025-00722-6

Zhao, L., Li, Z., & Qu, L. (2022). Forecasting of Beijing PM2.5 with a hybrid ARIMA model based on integrated AIC and improved GS fixed-order methods and seasonal decomposition. Heliyon, 8(12), e12239. https://doi.org/10.1016/j.heliyon.2022.e12239

U.S. Geological Survey. (2024). Landsat-9 imagery of Bangka Strait area [satellite image data]. EarthExplorer. Retrieved on February 27, 2025, from https://earthexplorer.usgs.gov

U.S. Geological Survey. (2025). usgs. https://.usgs.gov. Retrieved on July 17, 2025.

U.S. Geological Survey. (n.d.). *Landsat Collection 2 Level-2 science products*. U.S. Department of the Interior. Retrieved July 29, 2025, from https://www.usgs.gov/landsat-missions/landsat-collection-2-level-2-science-products